Original Article

SHM Structural Health Monitoring

Structural Health Monitoring
1–11

DOI: 10.1177/1475921716666411
shm.sagepub.com
SAGE

Characterization of delamination-type damages in composite laminates using guided wave visualization and air-coupled ultrasound

Rabi S Panda, Prabhu Rajagopal and Krishnan Balasubramaniam

Abstract

This article reports on the characterization of delamination damages in composite laminates using wave visualization method. A combination of plate-guided ultrasound and air-coupled ultrasonics is used to locate and visualize delaminations. The study focuses on the physics of Lamb wave propagation and interaction with delaminations at various through-thickness locations and positions. Three-dimensional finite element simulations are used to study, in detail, the changes in wave features such as mode velocity, wavelength and wave refraction in the delamination region. These wave features provide information on the location, position and orientation of the delamination. These studies are validated by experimental measurements. The influence of position of source and delamination on wave refraction in the delamination region is examined. This method also correlates the results obtained from experiments and finite element simulations to theoretical dispersion curves in order to distinctly determine the delamination location.

Keywords

Lamb waves, delamination, wave visualization, air-coupled ultrasound, non-destructive testing, structural health monitoring

Introduction

The usage of fibre-reinforced plastic (FRP) composite materials in aerospace, military and civilian structural applications has increased significantly due to attractive mechanical properties such as high specific strength and modulus. Arising due to faulty manufacturing or operational conditions such as impact or fatigue loading and temperature, delamination is a common damage type in composites that reduces the strength, stiffness and integrity of the structure. Delaminations are sub-surface damages and hence difficult to be detected and characterized, especially in the inaccessible/hidden regions of complex composite structures. Thus, composite materials require stringent non-destructive testing/non-destructive evaluation (NDT/NDE) techniques to ensure the overall integrity and reliability of the structures. Ultrasonic guided wave[1–4] methods are promising for rapid inspection of large areas of structure from a single transducer position.

Lamb waves are ultrasonic waves guided by geometrical boundaries of plate-like structures and can travel over a long distance with less attenuation. The entire thickness of the laminate can be interrogated by various Lamb modes,[3] allowing detection of surface and sub-surface damages. Hence, these waves can be used for NDE as well as structural health monitoring (SHM) of composite structures.[1,2] Damage detection in composite laminates utilizing Lamb waves requires understanding the physical principles of their propagation and interaction with damages. Over the last decade, studies on the interaction of Lamb waves with delamination-type defects have been reported by many researchers in composite laminates.[5–9]

Centre for Nondestructive Evaluation (CNDE), Department of Mechanical Engineering, Indian Institute of Technology Madras, Chennai, India

Corresponding author:
Rabi S Panda, Centre for Nondestructive Evaluation (CNDE), Department of Mechanical Engineering, Indian Institute of Technology Madras, 312 Machine Design Section, Chennai 600036, Tamil Nadu, India.
Email: rabisankarpanda@gmail.com

Of the various transduction methods available, air-coupled ultrasonic testing (AUT) technique is emerging as a promising method for non-contact inspection of composites.[7,10–12] The advantages of AUT include rapid automated scanning, excitation of a pure Lamb wave mode[11,13] and inspection of irregular and inaccessible regions. Non-contact inspection using Lamb modes to visualize damage in plate-like structures has been studied widely.[14–19]

This article investigates the physics of Lamb wave propagation and interaction with delamination-type defects in a quasi-isotropic composite laminate using a non-contact wave visualization approach (the method is highlighted in previous work by the authors; see Panda et al.[20] and Sasanka et al.[21]). The studies are carried out in the time domain, in view of simplicity and ease of practical implementation. This approach provides a series of images of propagating waves, which spans the scanned surface of the test piece. Wave features such as refraction to interaction with defects and changes to wave velocity and wavelength due to dispersion are recorded and exploited for detection of defects. The physics of wave refraction is shown to be the basis for delamination location in thickness direction of the laminate. Three-dimensional (3D) finite element (FE) simulations validated by experiments are used to study low-frequency A_0 mode interaction with square-shaped delaminations in glass-fibre reinforced plastic (GFRP) plate-like structures. The size of the delamination is chosen appropriately to capture changes to wave field when traversing the delamination regions. Qualitative results are followed by quantitative studies of the influence of various defect parameters on the visualized wave field.

The article is organized as follows. A brief background to the method used and problem studied is given in section 'Background'. The details of the experiments and 3D FE simulations carried out using air-coupled ultrasonic transducers are presented in section 'Methods'. Section 'Results and discussion' first presents results for experimental verification of FE simulation approach for the case of delamination located at a corner of the composite plate, with a discussion of physics of wave propagation and interaction with delaminations. Later on, the section presents results for delaminations located at the centre for the plate. The article concludes with directions for further work in section 'Summary and conclusions'.

Background

Lamb wave mode selection and excitation

Figure 1(a) and (b) shows the phase velocity and incident angle dispersion curves of Lamb waves travelling along 0° direction in the eight-layered quasi-isotropic GFRP composite laminate of 2.64 mm thickness. Here, we must clarify that, here and in the rest of this article, 'along 0° direction' means the guided waves travel along the fibre direction of 0° ply in the composite laminate. Dispersion curves are plotted using DISPERSE[22] software by considering the material properties and orientation of each individual ply as input data according to the layup of composite laminate. Low-frequency excitation of 100 kHz was considered in the study, to minimize the number of modes and wave attenuation in the received signal. This frequency range is also ideal for air-coupled ultrasonic inspection of composites. At such low frequencies, only the fundamental symmetric, S_0, and anti-symmetric, A_0, modes exist (see Figure 1(a)). The S_0 mode mainly consists of in-plane particle displacements, whereas the A_0 mode has out-of-plane particle displacements. On account of out-of-plane particle displacement, the A_0 mode can be measured conveniently with air-coupled ultrasonic transducer. Moreover, the A_0 mode has a shorter wavelength permitting study of smaller features. The A_0 mode was excited and received by appropriate positioning[11] of an air-coupled ultrasonic transducer (illustrated in Figure 2) based on Snell's law. From the incident angle dispersion curve shown in Figure 1(b), the receiving angle of A_0 mode at 100 kHz frequency was deduced to be approximately 21°.

Guided wave visualization approach

The presence of delamination causes a composite laminate to divide into two sub-laminates of reduced thicknesses. As can be seen from Figure 1(a), in the low frequency-thickness regime, the A_0 mode is dispersive. As the thickness decreases, the A_0 mode velocity decreases, thereby decreasing the wavelength. If this change in wavelength is measured, we can locate and visualize the defect region from outside. More details on the practical implementation of this approach in our work are given in the 'Results and discussion' section.

Problem studied

The article analyses GFRP composite laminates with engineered defects at various through-thickness locations (lamina interfaces) of the laminate to study Lamb wave propagation, detection and visualization of defects using the air-coupled ultrasonic technique (illustrated in Figure 2). The A_0 mode is excited in the laminate. Square-shaped delaminations, located at a corner of the laminates (illustrated in Figure 4(a)), are considered for the study. The position and through-thickness location of the defect are determined from the

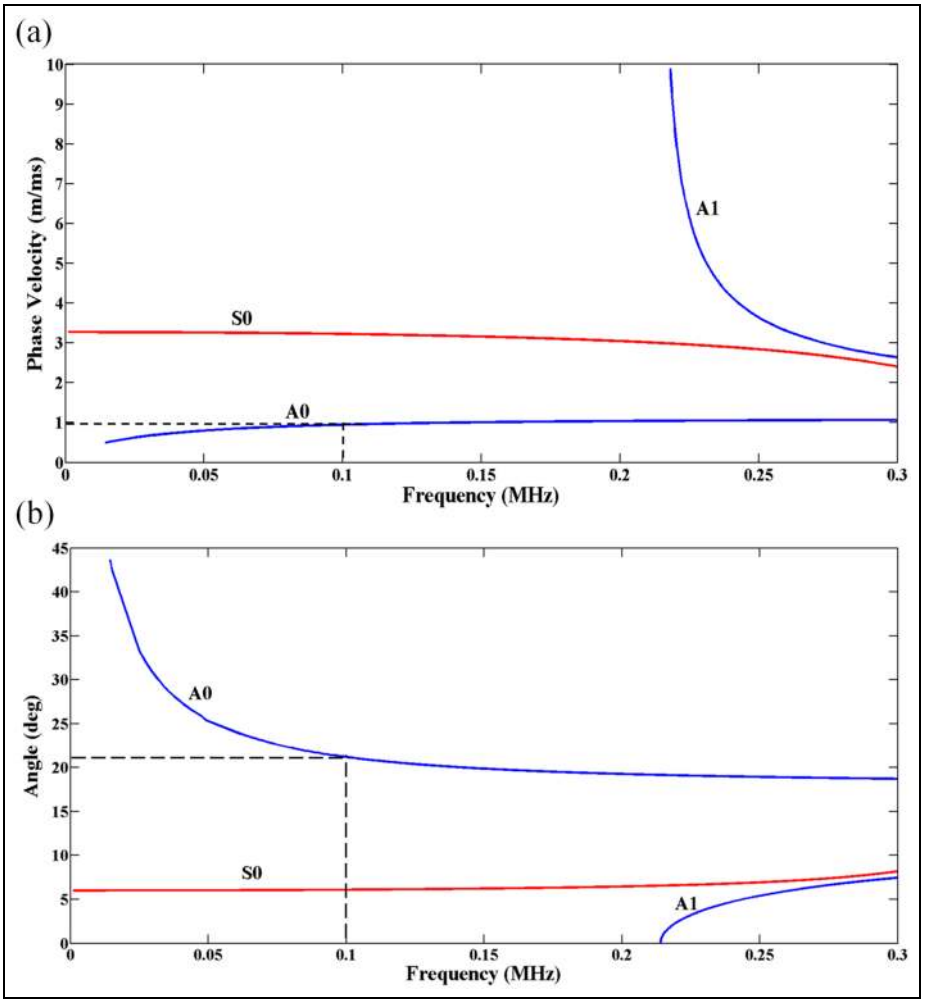

Figure 1. Plot showing (a) phase velocity dispersion curve and (b) incident angle dispersion curve.

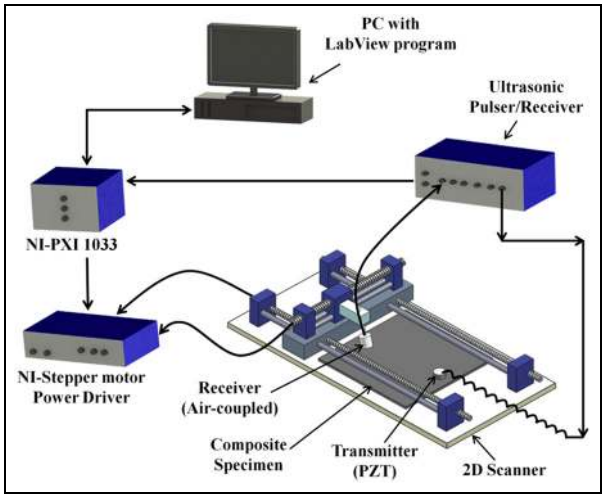

Figure 2. Schematic diagram of experimental setup.

interaction of the wave mode with the defect. First, we consider delaminations located at a corner of the plate: for this case, numerical (FE) results are validated with experiments since air-gap-type delaminations are more convenient to be created artificially. Based on thus validated FE models, we then study the case of air-gap delaminations located at the centre of the plate, where experimental samples are more difficult to create artificially. These numerical models are used to study the effect of defect position on wave scattering features. Details of physics of the problem are explained in the 'Results and discussion' section.

Methods

Procedure for experiments

Experiments were performed on eight-layered quasi-isotropic composite laminates of layup $[0/+45/–45/90]_S$

Table 1. Material properties of lamina.

E_{xx} (GPa)	E_{yy} (GPa)	ν_{xz}	ν_{yz}	G_{xz} (GPa)	ρ (kg/m^3)
44.68	6.90	0.28	0.355	2.54	1990

with delaminations at lamina interfaces in through-thickness locations. This type of ply layup is very commonly used in aerospace structures. The material properties of the composite laminates, as in Ramadas et al.,[9] are presented in Table 1. Thicknesses of each lamina and laminate were 0.33 and 2.64 mm, respectively. The size of each laminate was 300 mm × 200 mm with a square-shaped delamination of size 60 mm × 60 mm at one corner. A schematic of the laminate is shown in Figure 4(a). The presence of the delamination was confirmed using conventional ultrasonic air-coupled through-transmission C-scan.

The experiments were carried out in a custom-built C-scan-like setup, as shown in Figure 2. The experimental setup consists of a custom-built scanner, a pulser–receiver, a 100-MHz A/D card, a motion controller and a personal computer. A data acquisition and signal processing program was used to filter and average the captured data to improve the signal-to-noise ratio of the digitized signal. The pitch–catch arrangement was employed to generate and receive A_0 mode Lamb wave. A commercially available, adhesively bonded circular PZT crystal (Sparkler Ceramics Pvt. Ltd, http://www.sparklerceramics.com) of 12 mm diameter, 10 mm thickness and 100 kHz central frequency was used to excite the A_0 mode in the composite laminate. Here, we note that A_0 mode generation is a thickness-mode (thickness-dependent) phenomenon for the PZT crystal. Additionally, the impedance matching and the bonding quality of the PZT crystal are also important. Since in this study the interest is more in understanding the interaction of guided waves with the delamination, we did not optimize the crystal dimensions. A 100-kHz central frequency air-coupled transducer (The Ultran Group, USA, http://www.ultrangroup.com) of 25 mm diameter was used for measuring the out-of-plane displacement. The receiving angle of the transducer, based on the phase velocity of the A_0 mode, was calculated using Snell's law. The vertical position and angle of receiving transducer were adjusted manually. The air-coupled transducer was approximately 15 mm away from the laminate surface, corresponding to the best signal amplitude of the received wave mode.

The scanning was conducted for a specific area of 140 mm × 120 mm of the laminate, including the delamination region with a resolution of 0.5 mm × 0.5 mm by the moving air-coupled transducer. Lamb waves were excited and propagated in the composite laminate. The excitation signal was a 100-kHz narrow-band five-cycle sinusoidal tone burst pulse modulated by a Hanning window. The Lamb waves propagate in the laminate and leak to the surrounding air medium due to out-of-plane displacement of surface particles. These leaky Lamb wave[23] signals were collected at each data point, shown in Figure 3(a) as A-scans by a built-in data acquisition system. At a particular time instant, the displacement field was obtained from the collected A-scans as shown in Figure 3(b).

The time response at each measurement point was averaged 16 times to improve the signal-to-noise ratio. A 30- to 500-kHz band-pass filter was applied to limit the bandwidth of the output signal. The raw data contain time signals from each of the scanned points. The data were then exported to the MATLAB software

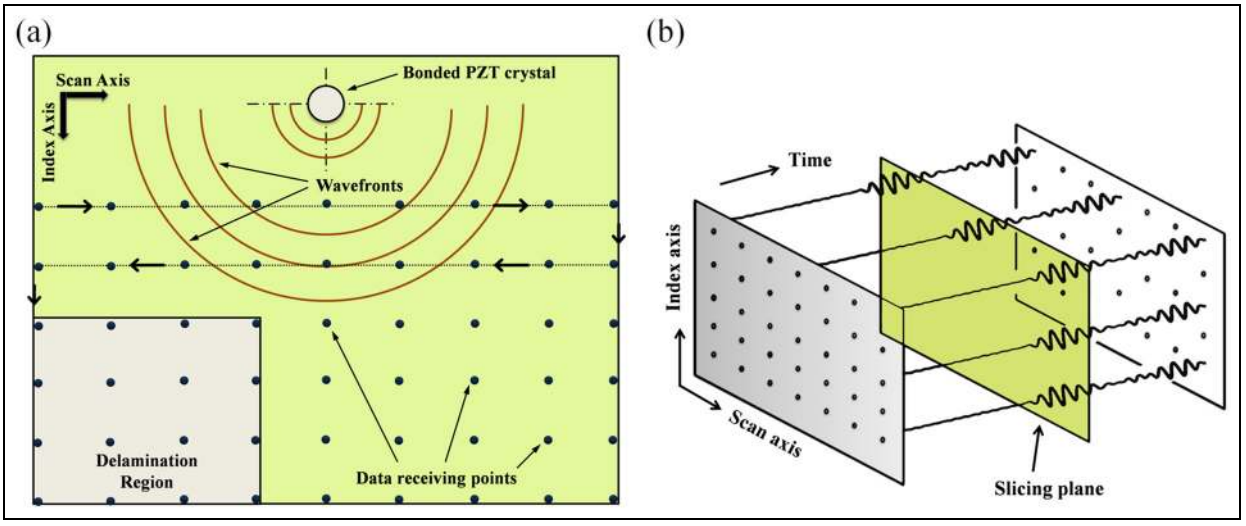

Figure 3. (a) A-scan receiving points and (b) displacement field at a particular time instant.

program and processed to get the out-of-plane displacement field across the scanned surface of the specimen at a particular instant in time. The resultant images from MATLAB were plotted as a two-dimensional (2D) colour image. The wave propagation in the laminate and the interaction with the delaminated region can be visualized from these images.

Procedure for 3D FE simulations

The 3D numerical simulations were carried out using commercially available FE package[24] on similar samples used in experiments to visualize the Lamb wave propagation and interaction with delamination. A schematic diagram of the configuration used in FE simulations is shown in Figure 4(a) and the ply layups in Figure 4(b). The dimensions of the composite laminates chosen were 150 mm × 120 mm × 2.64 mm, to avoid the early reflections from model boundaries and to minimize the total run time.

The lamina properties are the same as those used in experiments, and for simplicity, viscoelastic properties are not considered (see Table 1). In the numerical models, each lamina was modelled individually and properties were assigned depending on the layup. Each lamina was modelled using eight-noded 3D solid brick elements (C3D8R) having three degrees-of-freedom at each node. The incremental time step size and mesh element size of the FE simulations are of importance for the stability and the accuracy of the solution. The incremental time step size and element size were selected as stated, for example, in Ramdhas et al.[25] The size of the elements was 0.165 mm in the thickness direction and 0.25 mm in both length and width directions. The FE mesh ensures that at least 40 elements exist per A_0 mode wavelength to provide a converged solution for elastic wave propagation.[26] The incremental time step used was 0.01 μs. A 100-kHz narrow-band five-cycle sinusoidal tone burst pulse modulated by a Hanning window was used as the excitation signal. The A_0 mode was excited by applying the out-of-plane (along the *z*-direction) nodal displacement to the surface FE nodes at the edge of the laminate to avoid edge reflections as shown in Figure 4(a). The delamination region in the laminate was modelled by disconnecting the surfaces of adjacent layers imitating an air-gap. The region without delamination was connected to the adjacent layers, thus ensuring continuity of displacements in the numerical model. Without loss of generality, the delamination can exist at any through-thickness location between a pair of ply interfaces. The size of delamination considered was of 60 mm × 60 mm. Out-of-plane displacement was captured at the receiver location. Simulations were repeated by changing the delamination location along through-thickness of the laminate between a pair of lamina interfaces.

Results and discussion

Qualitative measurements

The results obtained from the experiment are presented in Figure 5. The images (see Figure 5(a) and (b)) show the A_0 mode wave propagation and interaction with delamination located between third and fourth layers of the laminate at various time instants.

Several characteristic changes such as the reduction in amplitude, change in wavelength, speed of propagation and deflection of wavefronts of the selected A_0 mode are observed at the delamination region. Since the delamination was created with air-gap between the

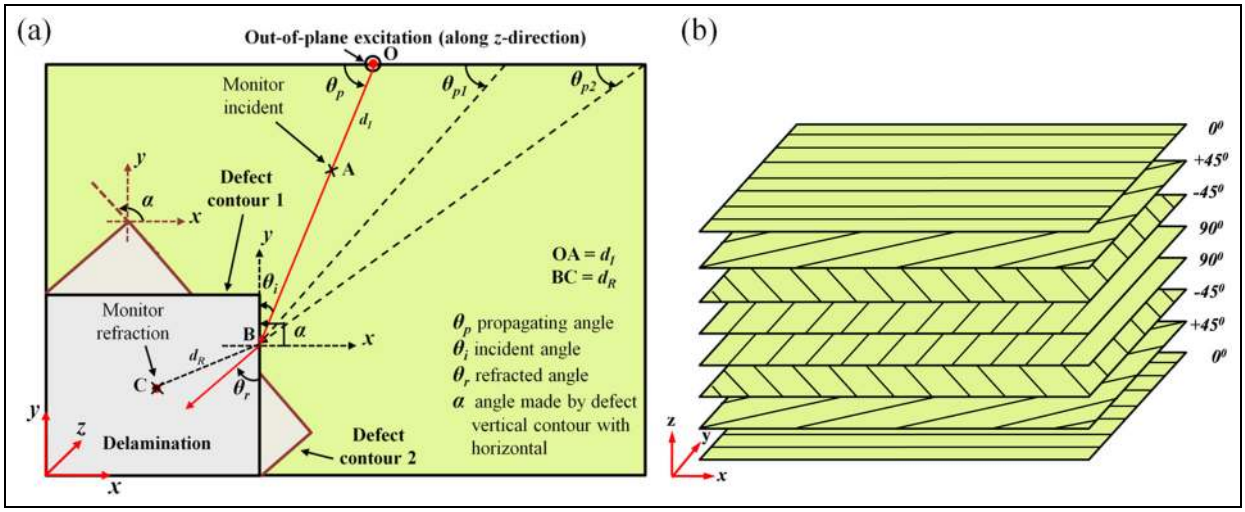

Figure 4. (a) Composite laminates with defect orientation and position and (b) ply layups.

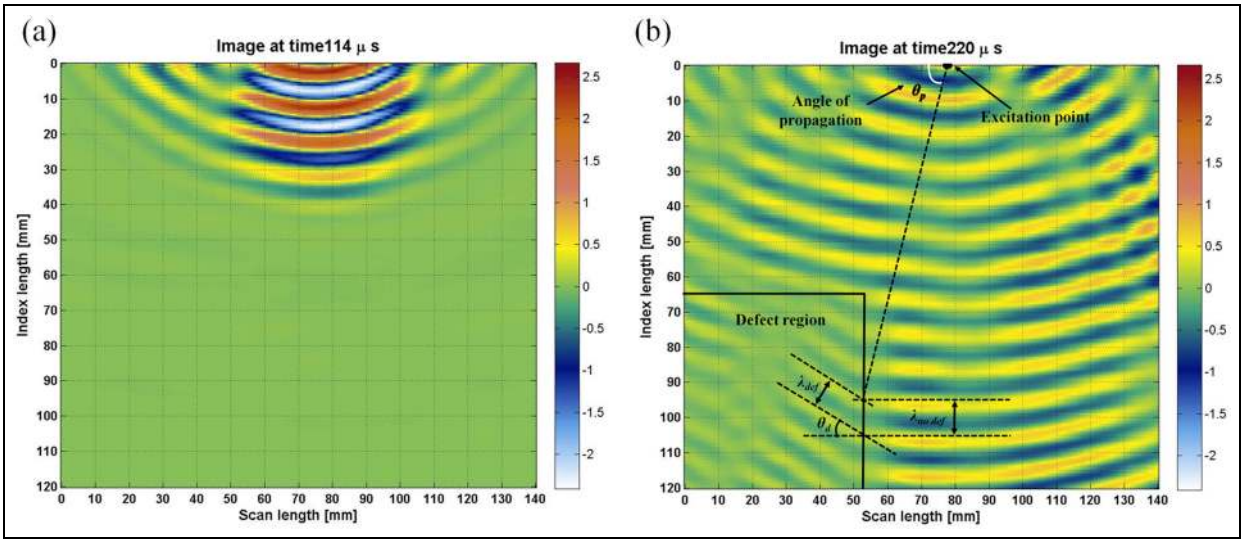

Figure 5. Experimental results showing the A_0 mode propagation and interaction with delamination between third and fourth laminas at different times: (a) 114 μs and (b) 220 μs.

layers, there was an impedance mismatch between the defective and healthy region. The impedance of air is much lesser than that of the laminate material. When the Lamb wave interacts with the delamination region, some of the energy is reflected back, some mode converted[9] into other modes and the remaining is transmitted into it. Therefore, wave amplitude is reduced in the delamination region as a result of reflection and mode conversion. Figure 5(b) does not show reflected energy because we received only the forward travelling A_0 mode, since we kept the air-coupled receiver at a particular angle, say +θ degrees with the normal (see Figure 2). To receive the backward travelling wave modes, that is, the reflection from the defect boundaries, we would have to keep the air-coupled receiver at –θ degrees with the normal (see Kazys et al.,[13] Figure 1(b), page e820). The mode-converted signal is also not shown in Figure 5(b), as in the present setup the receiving probe was set to pick only the A_0 mode. The wavelength change is affected by the velocity change. This is because the laminate is getting divided into two sub-laminates by the defect. The wavelength reduces in the thinner sub-laminate and it gradually increases as the sub-laminate thickness increases. The deflection of the wavefront occurs due to the mismatch in impedance between the healthy and defective region. In a healthy region, wave enters and leaves without leaving any traces of energy, while multiple reflections may occur in the defective zone due to the energy trapped[15] in it.

In FE simulations, the delaminations were created between a pair of lamina interfaces. The results obtained from FE simulations when A_0 mode wave interacts with delaminations at various through-thickness locations for a particular propagating angle, θ_p are shown in Figure 6. In this study, the propagating angle is defined as the angle between the top horizontal edge of the laminate and the line joining the point of loading/excitation to the intersection point of a wavefront with the vertical defect contour. The propagating angle was calculated for a certain time instant (see Figure 6(b)) and was fixed at 78°. This changes with time, and accordingly, the wave deflection θ_d can be calculated. These results, especially Figure 6(b), are in good agreement with those generated by the experimental wave visualization method, presented in Figure 5(b).

It was observed from the experiments and simulations that there is a strong correlation between the wave deviation and the location of delamination along the thickness of the laminate. The wave deviates from its original direction of propagation when it interacts with the defect. Application of Snell's law shows that a reflected wave and a refracted wave are expected in all cases, with the exception of normal incidence. The refracted wave bends towards or away from the normal depending on the velocity differences in healthy and defective regions of the laminate. As it is known that mode velocities vary with the position of defects, this phenomenon causes wavefronts to bend to different extents for defects in different depths. This suggests that studying the wave path deviations can provide information on the location of defective regions.

Quantitative measurements

Studies were conducted to check whether the wave field measurements can provide a quantitative guidance on the position and orientation of defects.

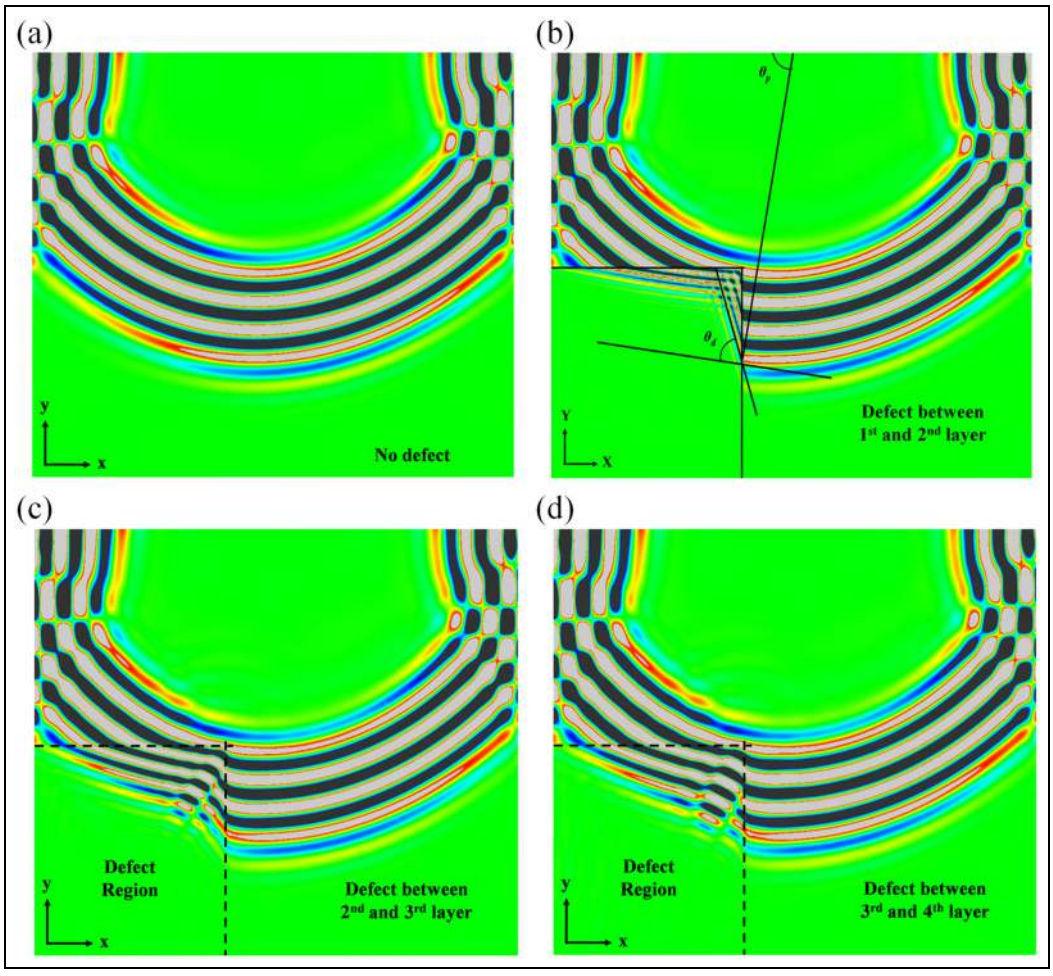

Figure 6. Contours of displacement magnitude as obtained from FE simulations at 96 μs for A_0 mode interaction with defects between different layers: (a) no defect, (b) one and two, (c) two and three and (d) three and four.

Angle of wave deflection θ_d *with through-thickness location of delamination.* The angle of deviation θ_d which is the wave deflected in the defective region for a particular propagating angle θ_p was calculated for various delamination locations along the laminate thickness. An example of the calculation of the wave deflection angle into the delamination is shown in Figure 6(b). Figure 7 shows the calculated values from FE simulations and average experimental values. We observe very good agreement between experimental results and FE predictions. This result shows that obtaining the wave deviation angle can provide a practical quantitative parameter to locate the delamination in the thickness direction.

The basis for the trend of the angle of deviation can be explained based on Snell's law

$$v_1 \sin\theta_1 = v_2 \sin\theta_2 \tag{1}$$

where v_1 and v_2 are the mode velocities in the healthy laminate and top sub-laminate, respectively, and θ_1 and θ_2 are the corresponding wave angles. Since in our study the value of v_1 and θ_1 are fixed, equation (1) shows that $\theta_2 \propto 1/v_2$, that is, the wave angle in top sub-laminate varies inversely with the wave velocity. As can be seen in phase velocity dispersion curve, Figure 1(a), the velocity of A_0 wave mode increases with laminate thickness. The top sub-laminate thickness increases with the location of delamination along the thickness direction, thereby increasing the wave velocity, and hence, the angle of deflection/refraction angle decreases. The location of the delamination in thickness direction of the laminate can be identified by measuring this refraction angle.

Wave refraction. As in Rajagopal and Lowe,[26] the wave refraction was studied in terms of the frequency domain ratio of the beam compensated refracted and incident signals, given as follows

$$\text{Refraction ratio} = \frac{R(\omega).\sqrt{d_R}}{I(\omega).\sqrt{d_I}} \tag{2}$$

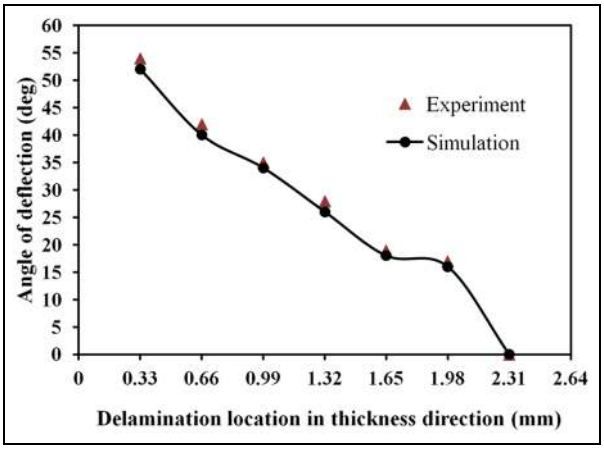

Figure 7. Variation of angle of wave deflection with delamination location in thickness direction.

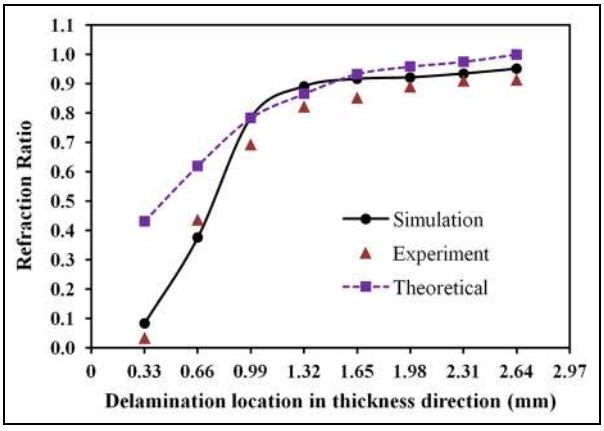

Figure 8. Variation of refraction ratio with through-thickness delamination location.

where $R(\omega)$ and $I(\omega)$ are the frequency spectra of the resultant displacement obtained from the refracted and incident signals, respectively; d_R is the distance from the refraction point to the point where the refraction is monitored; and d_I is the distance from the source to the point where the incident signal is monitored. (See, for instance, Figure 4(a) for an illustration.) Figure 8 shows average experimentally measured and FE predicted values of the refraction ratio for the monitored location, plotted with the through-thickness location of delamination.

The above trend of refraction ratio again follows based on the dispersive property of the A_0 mode. It was observed that the value of refraction ratio increases along the laminate thickness. Based on acoustic impedance, we can write, assuming plane wave behavior in the far-field,

$$\text{Refraction ratio} = \frac{2Z_2}{Z_1 + Z_2} \tag{3}$$

where Z_1 and Z_2 are the acoustic impedances of the healthy laminate and top sub-laminate, respectively. $Z = \rho v$, where ρ is the density of the material of the laminate and v is the wave velocity. Let v_1 and v_2 be the mode velocities in the healthy laminate and top sub-laminate, respectively. The density of the material of the laminate and sub-laminate is the same, that is, $\rho = \rho_1 = \rho_2$. Therefore, from equation (3)

$$\text{Refraction ratio} = \frac{2v_2}{v_1 + v_2} \tag{4}$$

When the top sub-laminate thickness is small, the wave velocity (v_2) is very low compared to the velocity in healthy region (v_1) and can be neglected in the denominator of equation (4). So it is clear from equation (4) that Refraction ratio $\propto v_2$, that is, the wave refraction directly varies with the wave velocity in the top sub-laminate. Figure 8 also shows values obtained for refraction ratio based on calculations in equation (4). The velocities for each sub-laminate were obtained from DISPERSE[22] for these calculations. We find good agreement with FE and experimental results.

As the top sub-laminate thickness increases with the location of delamination in successive laminas along the thickness of the laminate changes, the velocity and wavelength of the wave mode increase. (See the phase velocity dispersion curve, Figure 1(a).) Due to an increase in velocity in the top sub-laminate and transmission of more energy to the defect region, the value of refraction ratio increases along the laminate thickness. By finding this wave refraction value, we can predict the location of the delamination along the thickness of the laminate.

Velocity curves from dispersion. The presence of a delamination between a pair of laminas causes a laminate to divide into two sub-laminates. Behaviour of wave modes in sub-laminates can be understood from the dispersion properties of concerned mode. In an eight-layered laminate, the defect could be present after first, second or seventh layers. In these cases, dispersion properties of all layered combinations must be considered. In composites, dispersion properties change as propagating angle changes. The data were collected by plotting dispersion curves for various combinations of layers, such as single-layered, two-layered and up to eight-layered laminates (as in Table 2) at different propagation angles.

Using the data collected from disperse plots, the normalized velocity curves were generated for fundamental A_0 and S_0 modes. The maximum velocity

Table 2. Layer combinations.

Layers	Layup	Thickness (mm)
First	[0]	0.33
First and second	[0/+45]	0.66
First to third	[0/+45/–45]	0.99
First to fourth	[0/+45/–45/90]	1.32
First to fifth	[0/+45/–45/90/90]	1.65
First to sixth	[0/+45/–45/90/90/–45]	1.98
First to seventh	[0/+45/–45/90/90/–45/+45]	2.31
First to eighth	[0/+45/–45/90/90/–45/+45/0]	2.64

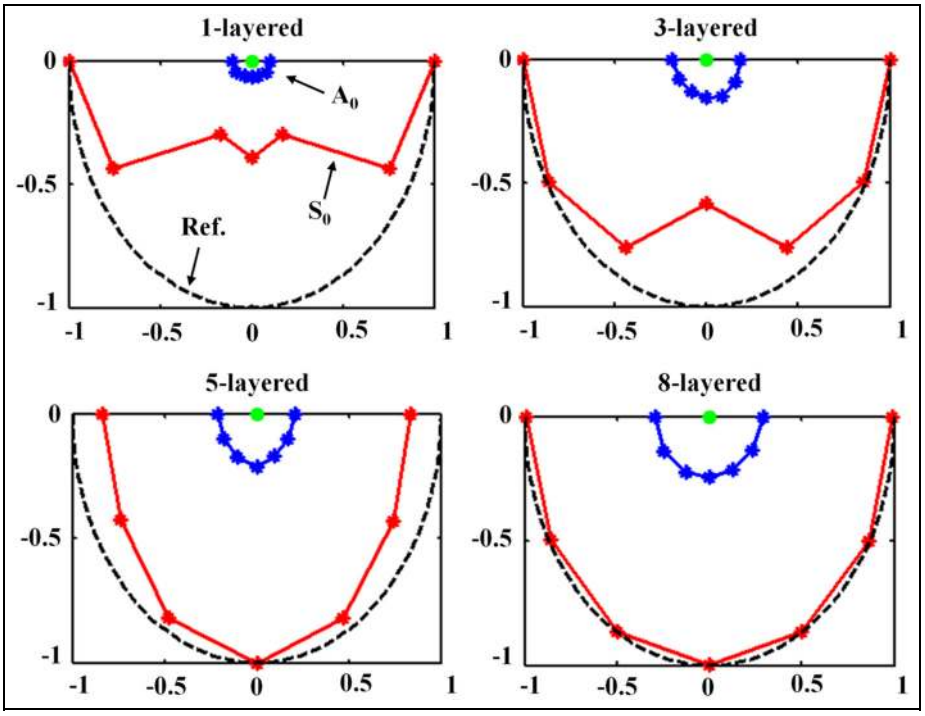

Figure 9. Normalized velocity curves for different layered combinations.

(V_{max} = 4767 m/s) among all velocities in different directions was taken to normalize them. A reference semicircle of unit radius was drawn to compare mode velocities with normalized velocity (V_n) at any angle. Figure 9 shows the normalized velocity curves for some of the layer combinations (sub-laminates), as given in Table 2. It was observed from the velocity curves that when the location of the delamination changes gradually from the first layer to eighth layer, the velocity and wavelength for a particular mode increase.

The studies mentioned so far in this article are focused on a single propagating angle θ_p and a particular position of the defect. For better understanding of this phenomenon, the study is extended to various propagating angles and different defect positions.

Change in wave features with defect position and propagating angle. The influences of the propagating angle on the angle of wave deflection in the defect region were also studied with the help of FE models. The delamination was modelled at the centre of the laminate as illustrated in Figure 10. The angle of wave deflection θ_d at the defect region was calculated for different propagating angles θ_p and through-thickness defect locations. The variation in angle of deflection with propagating angles and through-thickness defect locations are given in Table 3.

These studies demonstrate that the leaky guided wave scanning approach can provide effective visualization of defects in composite laminates, along with a guidance as to the location (and also possibly, the orientation) of defects along the thickness.

Table 3. Deflection values for different propagating angles.

Defect location (between layers)	Angle of propagation, θ_p (deg)			Angle of deflection, θ_d (deg)		
	θ_{p1}	θ_{p2}	θ_{p3}	θ_{d1}	θ_{d2}	θ_{d3}
First and second	75	62	47	52	48	34
Second and third	75	62	47	39	36	23
Third and fourth	75	62	47	32	29	18
Fourth and fifth	75	62	47	22	20	14
Fifth and sixth	75	62	47	17	16	09
Sixth and seventh	75	62	47	13	13	05
Seventh and eighth	75	62	47	07	06	04

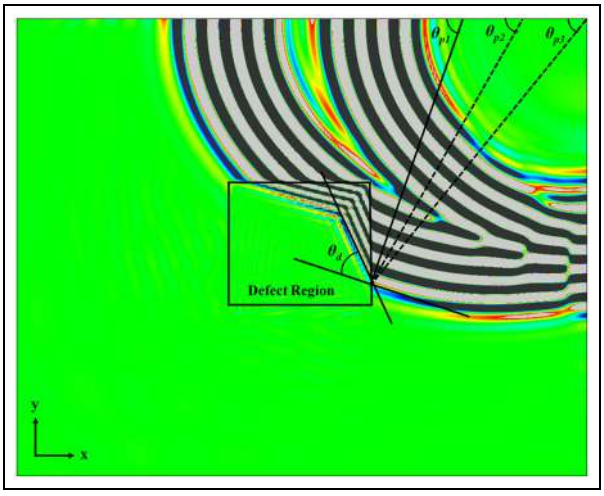

Figure 10. Displacement contour showing deflection of A_0 mode in defective zone (FE simulation).

Summary and conclusion

This article studied the A_0 mode Lamb wave propagation and interaction with delamination in a $[0/45/–45/90]_S$ quasi-isotropic composite laminate at the low-frequency regime using visualization approach. The acoustic wave field visualization images were generated with air-coupled ultrasonic technique using leaky Lamb waves. The investigation was carried out with 3D FE simulations and validated by experiments. FE simulations and experiments were conducted on quasi-isotropic laminates containing delaminations at various lamina interfaces across the laminate thickness. The results in both cases are in good agreement as shown in Figures 5 and 6. Also, quantitative parameters such as wavefront deflection and refraction ratio were measured at the delamination region to know the effectiveness of the selected method. The variability in the results obtained is due to the orientation of the receiving transducer, material attenuation and instrumental errors. Several characteristic changes of A_0 mode Lamb wave such as amplitude reduction, change in wavelength, speed of propagation and deflection of the wavefronts were observed in the defective region. It was also observed from the FE simulations that the wave refraction angle in the defective region varies with position of source and delamination (Figures 6(b) and 10), as given in Table 3. The correlation of the results obtained from experiments and FE simulations to theoretical dispersion curves validates the technique presented here.

The results of these studies provide improved physical insight into the wave interaction at delaminations at various depths across laminate thickness. The wave visualization approach using air-coupled ultrasound was found to be a useful tool for analysing the wave mode interactions with damages in composites. Guided Lamb wave modes can be used to locate and find the depth of a delamination by measuring the mode wavelength change and wave refraction angle in the delamination region. Non-contact inspection of composite laminates using air-coupled ultrasonic technique has advantages over laser-based and PZT film–based SHM. Laser-based sensing is not convenient for composite materials because of the low reflectivity, low sensitivity, high noise, high cost and single-point measurements. Similarly, PZT film–based Lamb wave sensing is intrusive and not accepted by the industry in many applications. The air-coupled receiver has better efficiency for measuring the A_0 mode because it integrates normal displacements over a surface corresponding to that of its field of view.[27] The findings are important to further advance this damage detection technique to complex structures.

Acknowledgment

The authors thank Mr DVS Sasanka for his assistance during experiments and helpful discussions.

Declaration of Conflicting Interests

The author(s) declared no potential conflicts of interest with respect to the research, authorship and/or publication of this article.

Funding

The author(s) disclosed receipt of the following financial support for the research, authorship, and/or publication of this article: The authors gratefully acknowledge support from the NPMASS program managed by The Aeronautical Development Agency (ADA) Bangalore, India.

References

1. Janardhan PM and Balasubramaniam K. Lamb-wave-based structural health monitoring technique for inaccessible regions in complex composite structures. *Struct Control Hlth* 2014; 21(5): 817–832.
2. Raghavan A and Cesnik CES. Review of guided-wave structural health monitoring. *Shock Vib Digest* 2007; 39(2): 91–114.
3. Rose JL. *Ultrasonic waves in solid media*. Cambridge: Cambridge University Press, 1999.
4. Su Z, Ye L and Lu Y. Guided Lamb waves for identification of damage in composite structures: a review. *J Sound Vib* 2006; 295(3–5): 753–780.
5. Guo N and Cawley P. The interaction of Lamb waves with delaminations in composite laminates. *J Acoust Soc Am* 1993; 94(4): 2240–2246.
6. Kessler SS, Spearing SM and Soutis C. Damage detection in composite materials using Lamb wave methods. *Smart Mater Struct* 2002; 11(2): 269–278.
7. Liu Z, Yu H, He C, et al. Delamination detection in composite beams using pure Lamb mode generated by air-coupled ultrasonic transducer. *J Intel Mat Syst Str* 2014; 25(5): 541–550.
8. Padiyar MJ and Balasubramaniam K. Quantitative characterization of interface delamination in composite T-joint using couplant-free Lamb wave methods. *J Reinf Plast Comp* 2016; 35(4): 345–361.
9. Ramadas C, Janardhan PM, Balasubramaniam K, et al. Delamination size detection using time of flight of anti-symmetric (Ao) and mode converted Ao mode of guided Lamb waves. *J Intel Mat Syst Str* 2010; 21(8): 817–825.
10. Bhardwaj MC. Phenomenally high transduction air/gas transducers for practical non-contact ultrasonic applications. In: *Proceedings of review of progress in quantitative nondestructive evaluation* (ed DO Thompson and DE Chimenti), Chicago, IL, 22–25 July 2008, vol. 1096, pp. 920–927. Melville, NY: AIP.
11. Castaings M and Cawley P. The generation, propagation, and detection of Lamb waves in plates using air-coupled ultrasonic transducers. *J Acoust Soc Am* 1996; 100(5): 3070–3077.
12. Michaels JE and Michaels TE. On the measurement of guided wavefields via air-coupled ultrasonic transducers. In: *Proceedings of review of progress in quantitative nondestructive evaluation* (ed DE Chimenti and LJ Bond), Boise, ID, 20–25 July 2014, vol. 1650, pp. 792–798. Melville, NY: AIP.
13. Kazys R, Demcenko A, Zukauskas E, et al. Air-coupled ultrasonic investigation of multi-layered composite materials. *Ultrasonics* 2006; 44: e819–e822.
14. Michaels TE, Michaels JE and Ruzzene M. Frequency–wavenumber domain analysis of guided wavefields. *Ultrasonics* 2011; 51(4): 452–466.
15. Park B, An YK and Sohn H. Visualization of hidden delamination and debonding in composites through non-contact laser ultrasonic scanning. *Compos Sci Technol* 2014; 100: 10–18.
16. Ramadas C, Padiyar J, Balasubramaniam K, et al. Lamb wave based ultrasonic imaging of interface delamination in a composite T-joint. *NDT&E Int* 2011; 44(6): 523–530.
17. Tian Z, Yu L and Leckey C. Delamination detection and quantification on laminated composite structures with Lamb waves and wavenumber analysis. *J Intel Mat Syst Str* 2015; 26(13): 1723–1738.
18. Tian Z, Leckey C and Seebo J. Guided wave imaging for detection and evaluation of impact-induced delamination in composites. *Smart Mater Struct* 2015; 24: 105019.
19. Yashiro S, Takatsubo J and Toyama N. An NDT technique for composite structures using visualized Lamb-wave propagation. *Compos Sci Technol* 2007; 67: 3202–3208.
20. Panda RS, Rajagopal P and Balasubramaniam K. An approach for defect visualization and identification in composite plate structures using air-coupled guided ultrasound. In: *Proceedings of review of progress in quantitative nondestructive evaluation* (ed DE Chimenti and LJ Bond), Boise, ID, 20–25 July 2014, vol. 1650, pp. 1299–1306. Melville, NY: AIP.
21. Sasanka DVS, Madhavan V, Padiyar MJ, et al. Visualization studies of Lamb wave propagation and interactions with anomalies in composite laminates using air-coupled ultrasonics. In: *Proceedings of review of progress in quantitative nondestructive evaluation* (ed DE Chimenti, LJ Bond and DO Thompson), Baltimore, MD, 21–26 July 2013, vol. 1581, pp. 1091–1097. Melville, NY: AIP.
22. DISPERSE user's manual, version 2.0.11, January 2016.
23. Chimenti DE and Martin RW. Nondestructive evaluation of composite laminates by leaky Lamb waves. *Ultrasonics* 1991; 29(1): 13–21.
24. ABAQUS analysis user's manual, version 6.12, January 2016.
25. Ramdhas A, Pattanayak RK, Balasubramaniam K, et al. Symmetric low-frequency feature-guided ultrasonic waves in thin plates with transverse bends. *Ultrasonics* 2015; 56: 232–242.
26. Rajagopal P and Lowe MJS. Short range scattering of the fundamental shear horizontal guided wave mode normally incident at a through-thickness crack in an isotropic plate. *J Acoust Soc Am* 2007; 122(3): 1527–1538.
27. Castaings M, Singh D and Viot P. Sizing of impact damages in composite materials using ultrasonic guided waves. *NDT&E Int* 2012; 46: 22–31.